Collisional excitation transfer in high magnetic fields. II.
Correlation function of the interaction in Hg(6³P₁)-Hg(6¹S₀) collisions

J. C. Gay and W. B. Schneider*

Laboratoire de Spectroscopie Hertzienne de l'E.N.S., Tour 12, Université Pierre et Marie Curie, 4 Place Jussieu, 75320 Paris Cedex 05, France †

(Received 6 July 1978)

The authors report results of the experimental study of excitation transfer between Zeeman sublevels of the 6^3P_1 state of an even isotope of mercury in magnetic fields up to 80 kG, obtained by monitoring the transition from sudden to partially adiabatic collisions. The results are shown to be in good agreement with theoretical evaluations based on a numerical solution of the relaxation problem or on a correlation-function description using a R^{-3} dipole-dipole interaction.

INTRODUCTION

We discuss the experimental study of excitation transfer between Zeeman sublevels of the 6^3P_1 state of an even isotope of mercury in magnetic fields of up to 80 kG. Here the energy separations due to the magnetic field are large enough for collisions to become somewhat adiabatic, with a corresponding decrease in cross section.

The principle of the experiments is to excite the 6^3P_1 $m = 0$ Zeeman sublevel of ^{198}Hg optically and to measure the rates of transfer towards the $m = \pm 1$ sublevels against the magnetic field.[1] Excitation transfer is observed through the polarization of resonance fluorescence reemitted by the vapor. As we continuously excite the $m = 0$ Zeeman sublevel, the resonance-fluorescence light must be totally π polarized in the low-pressure limit (with no interaction between atoms). At higher Hg pressures, depolarization of resonance radiation is caused by collision. The main difficulties in such experiments are the total elimination of parasitic effects: these are probably responsible for the relative failure of prior attempts.[2-5] Therefore we give here many details of the tests of the setup and physical justifications of the conditions of the study.

I. GENERAL EXPERIMENTAL CONDITIONS

A. Principle of experiments and choice of ^{198}Hg

Experiments have been performed on the 6^3P_1 state of mercury to study the magnetic field dependence of the excitation transfer by resonant ^{198}Hg-Hg* collisions from the $m = 0$ Zeeman sublevel (optically excited with a rf discharge lamp emitting the 2537-Å resonance line) to the $m = \pm 1$ sublevels.

The particular choice of the high-purity (99.7%) 198-even isotope of mercury for use in the experiments is made for several reasons. First, the $m = 0$ Zeeman sublevel is only weakly displaced by the field (see the Appendix). For $B = 80$ kG, the shift

of 0.21 GHz is small compared to the 2-GHz width of the excitation line. It is thus possible to excite it in strong magnetic fields (200 kG) with a rf discharge lamp containing the same isotope and placed in zero magnetic field. Moreover, the choice of an even isotope permits simplification of the experimental conditions, as there is no hyperfine structure. Second, as shown in the Appendix decoupling effects of $\vec{L}$ and $\vec{S}$ are negligibly small up to 200 kG. Such effects must be avoided, since they may be the origin of a parasitic field dependence arising in the transfer rates from modifications of the wave functions from their zero-field values. The modifications of the mixing of the 6^1P_1 and 6^3P_1 states due to the field, which may also modify the lifetime of the Zeeman sublevels of the 6^3P_1 state, are very small for fields of up to 200 kG. Diamagnetic shifts are also negligible. So, all *a priori* requirements seem well verified in the case of even mercury atoms, and an accurate experimental test of the theoretical predictions for $J = 1 \rightarrow J = 0$ transitions is possible.

B. Depolarization of resonance radiation and multiple scattering

To eliminate depolarization effects due to radiation trapping, it is sufficient to use magnetic field values such that the Zeeman splitting of the levels is several times greater than their Doppler width (about 2 kG in the present case). Under such conditions, multiple scattering becomes an anisotropic process[2,3,6] (the imprisonment times of the σ and π photons are different) and will not depolarize resonance radiation. Discarding instrumental depolarization, which may be easily deduced and corrected for, we consider only the depolarization of resonance radiation due to collisional processes.

C. Collisional processes in a cell

Excitation transfer comes from resonant Hg*-Hg collisions,[7-9] which is the process we investigate here. But it may also occur during the interaction

of an excited mercury atom with the walls of a cell or with another atom of a different species, one for which the collision process is nonresonant. Under our experimental conditions, the effects of interaction with the walls are negligible, but the interaction of Hg* with the residual gases contained in a sealed cell may not be. Some order of magnitudes may help to clarify the importance of this point. At $T = 300\,°K$, the mercury density is about 10^{13} atoms/cm³. The rate of transfer between the $m = 0$ and $m = \pm 1$ Zeeman sublevels[7-10] is $1.6 \times 10^{-3}\Gamma$, where Γ is the radiative-decay probability of the 6^3P_1 state. Suppose that the pressure of a residual gas X in the cell is about 10^{-3} Torr and that the gas is H_2O or He, for which the cross sections with Hg* are well known.[11] This gives $(m = 0 \rightarrow m \pm 1)$ transfer rates of about $0.6 \times 10^{-3}\Gamma$, i.e., of the order of magnitude of those of resonant Hg-Hg* collisions. The resonant Hg-Hg* contribution is rapidly field varying, while that of Hg*-X is not, since the collision time is several times shorter.[10,12] The apparent variations with the field observed under these conditions will then be weaker, as the variations for resonant collisions will be partly masked by the contribution of residual gases to the excitation transfer. It is thus essential that sealed cells containing at most 10^{-4} Torr residual gases be used, which turns out to be one of the major difficulties of the experiments.

D. Order of magnitude of magnetic fields

The collision time T_c may be defined phenomenologically as

$$T_c = (1/v)(\sigma/\pi)^{1/2}, \tag{1}$$

where σ is, for example, the cross section for the $(m = 0 \rightarrow m = \pm 1)$ excitation transfer in zero field ($\sigma = g/Nv$, where g is the transfer rate). The condition for which evolution of the atoms during collision is strongly perturbed by the magnetic field is given by

$$\omega T_c > 1, \tag{2}$$

where ω is the Larmor frequency. Relation (2) expresses the fact that during the collision time the $\vec{J}$ angular momentum of the system rotates through 2π radians around $\vec{B}$. As T_c^{-1} is also the width of the Fourier spectrum of the correlation function of the potential, condition (2) also means that the Fourier components able to produce the excitation transfer between the sublevels separated by $\hbar\omega$ are decreasing in amplitude. Then, for fields such that

$$B > B_c = (g_J \mu_B T_c)^{-1}, \tag{3}$$

the $(m = 0 \rightarrow m = \pm 1)$ excitation transfer rate $g^{\pm 10}$ may

begin to decrease. For Hg*(6^3P_1)-Hg(6^1S_0) collisions, T_c is about 10^{-11} sec, $\Gamma = 8.55 \times 10^{-6}$ sec⁻¹, and $g^{\pm 10} \sim 1.6 \times 10^{-16}\Gamma N$. Therefore B_c is about 10 kG. This rather small value of B_c is connected with the rather long collisions time and big cross sections of resonant collisions. In order to observe the saturation $(\omega T_c \gg 1)$ of the phenomena, fields five to ten times greater than the critical field B_c are needed. So the experimental evidence of such effects requires the use of superconductive or Bitter coils. In the present case fields up to $8B_c$ were used.

E. Order of magnitude of physical signals

In studies of relaxation by resonant collision, it is well known that when the effects of collisions are measurable, radiation trapping is also important. Various methods have been used in past years to separate these two phenomena for studying resonant collisions: the study of an isotope at a weak concentration in another one,[7] the use of elements with low-lying metastable states,[13] and the study of backscattered fluorescence light.[14,15] These methods are not used in our experiments, as they generally require very complicated interpretations in the 0–10-kG range, where interpretation is already complicated by the 25% variation of the transfer rates with the field predicted theoretically. We thus use no tricks to eliminate multiple scattering, but work in the strong-field regime (Zeeman splitting greater than Doppler width) where it does not produce any depolarization effects.

At fixed mercury density, radiation trapping plays the important role of amplifying the signal due to collisional transfer, since the collisional rate competes with the radiative loss rate. Indeed, in the limit of $g/\Gamma^\sigma \ll 1$ the ratio I_σ/I_π of the fluorescence intensities is just[2,6]

$$I_\sigma/I_\pi \sim g^{10}/\Gamma^\sigma, \tag{4}$$

where Γ^σ is the inverse of the imprisonment time of σ photons in the vapor and g^{10} the $(m = 0 \rightarrow m = \pm 1)$ collisional transfer rate. For $N = 2 \times 10^{13}$ at./cm³, the evaluation of Γ^σ with Holstein's model[16] gives $\Gamma/\Gamma^\sigma \sim 15$. As $g^{10} \sim 3.4 \times 10^{-3}\Gamma$, it follows that I_σ/I_π is about 0.05 and easily measurable. Since only the variation of g^{10} with the field is being measured, a precise value of Γ/Γ^σ is not important. That Γ/Γ^σ is independent of the field in the experimental range of fields is verified below. Equation (4) is correct only if backtransfer terms (transferring the excitation from $m = \pm 1$ to $m = 0$) are small, implying that
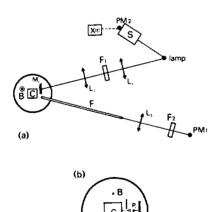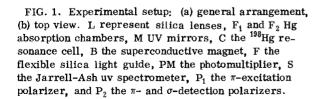
$$\Gamma^\sigma \gg g^{10}. \tag{5}$$

Performing the experiments at Hg densities where (4) holds is of interest, since I_o/I_π depends linearly on the transfer rate g^{10}. At the opposite extreme, if $\Gamma^o \ll g^{10}$ Zeeman populations become thermalized. Then I_o/I_π is constant and does not give any information on the collisional process.

To conclude, several conditions have to be fulfilled for convenient investigation of the field dependence of the $(m = 0 \rightarrow m = \pm 1)$ transfer rates in resonant Hg*-Hg collisions. The range of mercury densities must be between 10^{13} and 3×10^{13} at./cm³. For smaller densities the effect of 10^{-4} Torr residual gas will not be negligible compared to Hg-Hg* contribution at strong fields: for higher densities I_o/I_π will not be a linear function of the transfer rate. Of course, fields greater than 2 or 3 kG are also needed to avoid any depolarization effect from multiple scattering.

II. EXPERIMENTAL SETUP

The experimental setup is basically analogous to that used during earlier investigations of the variations of resonant-collision cross sections with magnetic field,[2,4,6] and is shown in Figs. 1. The 80-kG superconductive magnet with vertical axis and 7-cm clear bore is solenoidal. Measurements of the inhomogeneity of the field have given the value 4.4×10^{-3} in a 2-cm sphere that encompasses the experimental cell. Then, at 80 kG, the variation of the field in a 2-cm sphere around the center is about 320 G. Measurements have also been made at 3 cm from the center of the magnet on the axis, and give a value of 5.5×10^{-2} for the inhomogeneity.[6] The stray field at 3 m from the center is approximately dipolar and is 6 G for 80 kG.

The mercury cell and the optics (mirrors and polarizers) are placed on a cylindrical support inside the bore of the magnet, at room temperature. The excitation light emitted by the rf discharge lamp is focused on the cell by means of two silica lenses and two uv mirrors (each mirror deflects the beam through a right angle). It passes through a slit and a π polarizer placed close to the cell. The fluorescence light is detected at right angles to the excitation and field directions with a polarizer which can be oriented in π or σ positions. A slit is used to reduce both parasitic light and the inclination of the detection beam to the optical axis of the system. Then a fused-silica fiber conducts the light to a uv photomultiplier. Various absorption cells filled with high-purity isotopic mercury can be interposed in the light beams.

The electrodeless rf discharge lamp, of a classical type, is a 2-cm-diam disk of fused silica excited with a 2-GHz discharge. It contains ^{198}Hg (99.7% purity from mass separation) and about 3 Torr argon. The stability of the emission at 2537 Å is recorded by means of a Jarrel-Ash uv spectrometer and a uv photomultiplier.

The resonance cells are 2- or 2.5-cm fused-silica cubes with long tails, and have temperatures stabilized to within 0.1 ℃ by a thermostat. The vapor pressure of ^{198}Hg is monitored by the temperature of the tail, which may be varied from −40 to +20 ℃. The cubic part of the cell is maintained at 25 ℃ by an air-circulating system. The polarizers are W58-Käseman films which absorb strongly but have good rejection rates.

The photomultiplier is a 6256-B EMI which is shielded by several ARMCO iron cylinders and six Mumetal (1 mm thick) shields. The shield is designed to bear a 50-G stray field without any saturation effects. The σ and π signals are measured with a digital voltmeter which also records other information such as thermocouple emf's and the intensity in the coil.

(a)

(b)

FIG. 1. Experimental setup: (a) general arrangement, (b) top view. L represent silica lenses, F_1 and F_2 Hg absorption chambers, M UV mirrors, C the ^{198}Hg resonance cell, B the superconductive magnet, F the flexible silica light guide, PM the photomultiplier, S the Jarrell-Ash uv spectrometer, P_1 the π-excitation polarizer, and P_2 the π- and σ-detection polarizers.

III. THEORETICAL INTERPRETATION OF SIGNALS

The analytical expression of the fluorescence intensities I_σ and I_π can be deduced from the master equation for the density matrix and from additional assumptions on multiple scattering which are discussed in Ref. 6.

A. Master equation for density matrix

The master equation for the density matrix ρ of the excited $J = 1$ atoms can be written

$$\dot{\rho} = -i[\mathcal{H}, \rho] - \Gamma\rho - \langle M \rangle_c \rho + D\rho + (d\rho/dt)_p, \quad (6)$$

$\mathcal{H}$, $\langle M \rangle_c$, and D being respectively the Zeeman Hamiltonian and the operators on Liouville space which describe the effects of collision and multiple scattering; Γ is the radiative decay probability and $(d\rho/dt)_p$ the pumping term. Equation (6) involves several approximations, as it implicitly supposes that ρ does not depend on $\vec{r}$ and $\vec{v}$ and that D has a local expression. It also supposes that the coupling between multiple-scattering and collision effects is negligible. We suppose in the following that we are in the strong-field regime for multiple scattering. One then has, with obvious notations,

$$(D - \Gamma)|m\rangle\langle m| = -\Gamma^m |m\rangle\langle m|, \quad (7)$$

Γ^m being the inverse of the imprisonment time of the excitation in the m Zeeman sublevel with, from symmetry considerations,

$$\Gamma^1 = \Gamma^{-1} = \Gamma^\sigma, \quad \Gamma^0 = \Gamma^\pi.$$

From the properties of $\langle M \rangle_c$ demonstrated in Ref. 10 for resonant collisions one can write

$$\langle M \rangle_c |p\rangle\langle p| = \sum_m g^{mp}|m\rangle\langle m|, \quad (8)$$

with

$$\sum_m g^{mp} = 0$$

and

$$g^{mp} = g^{pm} = g^{-p-m} \quad (9)$$

if the field is sufficiently small to allow neglect of detailed balance corrections to (9).[17]

Projecting (6) onto the dyadic Zeeman basis leads to

$$\dot{\rho} = 0 = -(\Gamma^m + g^{mm})\rho_m + \sum_{p \neq m} |g^{mp}|\rho_p + A_m, \quad (10)$$

where A_m is the source term for the m Zeeman sublevel. We then explicitly obtain

$$\rho_0 = (\Gamma^\sigma + g^{10})/[\Gamma^\sigma\Gamma^\pi + g^{10}(2\Gamma^\sigma + \Gamma^\pi)], \quad (11)$$

$$\rho_{\pm 1} = g^{10}\rho_0/(\Gamma^\sigma + g^{10}).$$

When $\Gamma^\sigma, \Gamma^\pi \gg g^{mp}$ (small pressures) one has

$$\rho_0 \cong (\Gamma^\pi)^{-1}, \quad \rho_{\pm 1} \cong \rho_0 g^{10}\Gamma^\sigma, \quad (12)$$

and when $\Gamma^\sigma, \Gamma^\pi \ll g^{mp}$ (high pressure) (11) gives

$$\rho_0 \sim \rho_{\pm 1} \cong 1/(2\Gamma^\sigma + \Gamma^\pi) = \text{const}, \quad (13)$$

which expresses thermal equilibrium (with $\hbar\omega \ll kT$).

B. Expression for fluorescence intensity

The expressions for the intensities reemitted by the vapor depend strongly on the imprisonment of resonance radiation and thereby on the excitation distribution in the cell, on the spectral profile of the excitation light, on vapor-pressure conditions in the cell, and on the relative geometry of the beams and field. The simplest analytical model for calculating the intensities is developed in,[2,6] and is consistent with both Monte Carlo simulations[6,18] and with experimental results. It gives

$$I_m = \lambda^{(m)}(N)\rho_m, \quad (14)$$

where $\lambda^{(m)}(N)$ depends on the particular conditions of the study (density, distribution of excitation, size of cells) but not on collisions or on the magnetic field, and ρ_m is just the mean population of the m sublevel in the cell.

The expression for the ratio $\rho(N, B)$ of the fluorescence intensities is then

$$\rho(N, B) = \frac{I_\sigma}{I_\pi} = \frac{\lambda^{(\pm 1)}(N)}{\lambda^{(0)}(N)} \frac{\rho_{\pm 1}}{\rho_0} = \lambda(N)\frac{g^{10}}{\Gamma^\sigma + g^{10}}. \quad (15)$$

The value of $\lambda(N)$ [see Ref. (6)] is in general about 1. The limiting cases of (15) are of interest. If $\Gamma^\sigma, \Gamma^\pi \ll g$, I_π is almost constant and independent of the field value, while I_σ depends linearly on g^{10}, and decreases with the field[10]

$$\rho(N, B) \sim [\lambda(N)/\Gamma^\sigma(N)]g^{10}. \quad (16)$$

For high pressures $(\Gamma^\sigma, \Gamma^\pi \gg g^{10})$ I_σ and I_π depend neither on g nor on the field strength. One has then

$$\rho \sim \lambda(N). \quad (17)$$

These two very simple conclusions are well verified by experimental data, demonstrating the validity of the above-mentioned assumptions in the density range of the experiments.

IV. TESTS AND CORRECTIONS OF DATA

Some of the order-of-magnitude discussions in Sec. I show the importance of carefully checking the background gas levels in the cells, of the depolarization by optics, and also demonstrate the validity of the model of Sec. III. As the σ and π signals are analyzed by their polarization, it is necessary to be sure that their spectral compositions really correspond to emission by either the $m = 0$ or the $m = \pm 1$ Zeeman sublevels of the atoms in the cell. Since the detection polarizer is not perfect (because of the finite aperture of the detection beam), one has to correct the data for this imperfection. The main techniques which have been used for these purposes (Fig. 2) are magnetic scanning[19] and absorption by filters filled with various isotopes and placed in the detection or excitation beams.
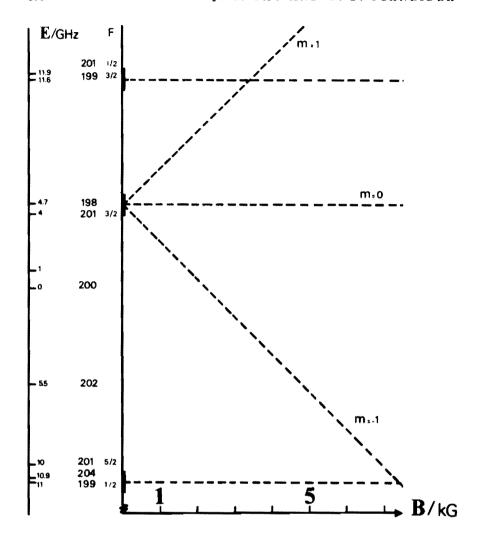
FIG. 2. Isotopic structure of mercury ($6\,^3P_1$ state) and principle of magnetic scanning methods. The energies of the hyperfine components of Hg are given on the left. The principle of the magnetic scanning method as performed on a ^{198}Hg cell with an ^{199}Hg filter in zero field is shown on the right-hand side.

A. Spectral composition of excitation light

All possibilities of direct excitation of the $m = \pm 1$ Zeeman sublevels of the atoms in the cell must be avoided, as they give rise to a parasitic contribution to the I_σ signal. By using a ^{204}Hg absorption chamber on the excitation beam and by sweeping the field on the cell around 7 kG (crossing of the $m = -1$ sublevel of ^{198}Hg with the line of ^{204}Hg in zero field), we have verified that there are no direct-excitation effects due to ^{204}Hg at a low concentration in the lamp, continuous background, or possible molecular bands of weak intensity emitted by the lamp. The absorption signal connected with possible direct-excitation effects is in all cases (with various filters) no more than 10^{-3} of the I_σ signal at densities of 2×10^{13} at./cm^3. Of course, since the width of the lamp line is equivalent to about 1 kG, direct excitation of the $m = \pm 1$ sublevels by the wings of the ^{198}Hg line is avoided at the stronger field values ($B > 3$ kG). Such ef-

fects are in all cases reduced by the π polarizer in the excitation beam. We have also carefully verified that isotopic impurities in the lamp (^{199}Hg is the main one) are negligible. The use of low-isotopic-purity samples as in Ref. 20 would not permit any quantitative interpretation of the data between 3 and 10 kG.

B. Polarizer imperfections

The π polarizer in the excitation beam serves essentially to reduce parasitic light and direct excitation of the $m = \pm 1$ levels. The imperfection of the detection polarizer is due to the finite angular aperture (20°) of the detection beam. The σ signal is then mixed with about 5% of π light. Writing R_σ and R_π for the measured signals for σ and π positions of the polarizers, I_σ and I_π for the true values of the fluorescence intensities emitted by the $m = \pm 1$ and $m = 0$ sublevels with the spectrum $k_0 \pm \omega$ and k_0, and α and β for the polarizer leakages, one

has

$$R_\sigma = I_\sigma + \alpha I_\pi , \quad R_\pi = I_\pi + \beta I_\sigma \simeq I_\pi , \qquad (18)$$

as the experimental conditions are such that $I_\sigma \ll I_\pi$. Then

$$R_\sigma / R_\pi = I_\sigma / I_\pi + \alpha . \qquad (19)$$

The value of α has been determined accurately by two methods based on the different spectral compositions of I_σ ($k_0 \pm \omega$) and I_π (k_0).

1. Use of ^{198}Hg absorption cells

Absorption of the k_0 component of R_σ, and thus measurement of R_π, R_σ, and I_π, is permitted by the presence of ^{198}Hg absorption cells in the detection beam. By having the cells's cold points either at room temperature or in liquid nitrogen, one can turn this R_σ absorption on or off. One then deduces α with good accuracy after correction of the effects of the parasitic light of the lamp (less than $10^{-2} I_\sigma$). This has been done under various conditions of temperatures and magnetic field with several kinds of absorption chambers (pure ^{198}Hg and ^{198}Hg with 60 Torr hydrogen). The values of α are fairly constant with the field, demonstrating that magneto-optical effects are negligible under our experimental conditions. For the conditions of the experimental observations reported below we obtain

$$\alpha = 0.051 \pm 0.001 . \qquad (20)$$

2. Magnetic scanning

A second method (the principle of which is recalled in Fig. 2) has been used to obtain an evaluation of systematic errors in (20). In the detection beam we use absorption chambers filled with an isotope different from ^{198}Hg. The value of I_σ in (18) is then determined by sweeping the field on the cell around the value for the crossing in energy of the components $k_0 - \omega$ or $k_0 + \omega$ of ^{198}Hg with the absorption line of the isotope contained in the filter (in zero field). The absorption signal is then simply proportional to $I(m = -1)$ or $I(m = 1)$ when the absorption is total, the other component being obtained by reversing the field. We have thus verified that

$$I(m = +1) \simeq I(m = -1) \simeq \tfrac{1}{2} I_\sigma (10^{-2}) , \qquad (21)$$

where 10^{-2} is the relative error. The use of odd isotopes of Hg permits the determination of both $I(m = -1)$ and $I(m = 1)$ by sweeping the field between 2 and 10 kG. In the situation illustrated in Fig. 2, two absorption signals are recorded for field values corresponding to the crossing of the $m = +1, -1$ Zeeman components of ^{198}Hg with the $F = \tfrac{3}{2}, \tfrac{1}{2}$ hyperfine components of ^{199}Hg in

zero field. We then obtain I_σ / I_π and (by putting the cold point of the filter in liquid nitrogen) R_σ / R_π. Finally, this yields

$$\alpha = 0.049 \pm 0.002 . \qquad (22)$$

3. Conclusions

The above techniques permit accurate determination of α, which is necessary in our experiments. But we have also verified that σ and π fluorescence have the correct frequency spectrum ($k_0, k_0 \pm \omega$) and that no parasitic contribution exists in the σ and π rays, such as stray light diffused on the walls of the cell or molecular bands coming from the strong absorption of some parts of the optics. One can thus conclude that the I_σ intensity is really due to the ($m = 0 \rightarrow m = \pm 1$) collisional excitation transfer in the cell.

C. Cell tests-residual gases

The cells are filled by fractional distillation of a high-purity mercury sample after 12-h of baking at 900 ℃. During these two operations they are connected to a high-vacuum pumping line. During the sealing operations the use of any trapping system (for freezing mercury atoms and avoiding great losses) is proscribed, since the main result would be to trap impurities in the cell (especially H_2O vapor desorbed by the heated silica).

Two kinds of tests have been performed. The first one is to verify that the isotopic impurities in ^{198}Hg have only unimportant effects on the σ signal; this has been verified with magnetic scanning. The second one is to measure the pressure of residual gases in the cell.

1. Residual-gas effects

We give in Fig. 3 two records obtained at the same Hg density with two cells having the same characteristics but with different (10^{-4} and 2×10^{-3} torr) residual-gas pressures. They show the same general behavior with the field but for the fact that the absolute values of I_σ / I_π are very different. The two curves are identical to a good approximation but for a translation independent of B.

2. Expression of the I_σ / I_π signal

The effects of residual gases on the excitation transfer are similar to those of resonant collisions. Relation (16) then becomes

$$I_\sigma / I_\pi = (\lambda / \Gamma^\sigma)(g + g^{10}) , \qquad (23)$$

where g is the ($m = 0 \rightarrow m = \pm 1$) transfer rate due to residual gas. Constant with N, g does not vary with B, as the collision time associated with these
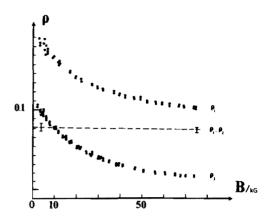
FIG. 3. Variations with B of $\rho = I_\sigma/I_\pi$ for two cells containing different residual-gas pressures (ρ_1: $g/\Gamma \sim 2\times10^{-3}$ and ρ_2: $g/\Gamma < 10^{-4}$). The data have been obtained at the same mercury density ($N = 1.7\times10^{13}$ at./cm³) and under the same geometrical conditions. The difference $\rho_1 - \rho_2$ of the values is almost constant with the field.

nonresonant interactions is shorter than that associated with resonant collisions. To use (23), it is then important to determine g or to adopt conditions such that $g \ll g^{10}$, where[7,10]

$$g^{10} = 1.6\times10^{-16}\Gamma N \qquad (24)$$

is the $(0 \rightarrow \pm1)$ transfer rate for resonant collisions.

An estimation of Γ^σ can be made using Holstein's model, which is not totally appropriate but gives good orders of magnitude. For $N = 2\times10^{13}$ at./cm³, the absorption coefficient $\chi(k_0)$ at the center of the line is 12 cm⁻¹ and the Holstein's expression for an infinite slab of thickness L is

$$\Gamma/\Gamma^\sigma = \chi(k_0)L\{\pi\ln[\chi(k_0)^{\frac{1}{2}}L]\}^{1/2}/1.9 , \qquad (25)$$

giving, with $L = 1$ cm, $\Gamma^\sigma/\Gamma \sim 0.07$. Using (16) and (24), one obtains $I_\sigma/I_\pi = 0.05$ with $g^{10} \ll \Gamma^\sigma$.

For a 10^{-3} Torr residual-gas pressure (for e.g., helium), g/Γ is 6.10^{-4}, about an order of magnitude less than g^{10}. When the field is between 3 and 80 kG, g^{10} decreases by about a factor of 3,[10] and a major contribution to excitation transfer at strong field will be due to residual gas. The effect will be an apparent reduction in the total variations of the rates with the field. One then has to use sealed cells for which

$$g/\Gamma < 10^{-4} \qquad (26)$$

in order to realize the experiments between 10^{13} and 3×10^{13} at./cm³. Higher mercury densities cannot be used owing to the condition $\Gamma^\sigma \gg g^{10}$ for the linearity of I_σ/I_π as a function of g^{10}.

3. Cell tests

The effect of residual gases is measured from the excitation transfer rates observed at low mercury densities. For $N = 10^{11}$ at./cm³, one has

$$I_\sigma/I_\pi = (g^{10}+g)/\Gamma \simeq g/\Gamma , \qquad (27)$$

since multiple scattering is almost negligible at these Hg densities, and $g^{10}/\Gamma \simeq 10^{-5}$. In the absence of residual gases the fluorescent light at low temperature is totally π polarized and $I_\sigma/I_\pi \simeq 0$.

In fact, measurements done on various cells show a typical 10^{-3} residual depolarization at low temperature (after correction for the imperfection of the polarizer). As this is a rather small value, it is necessary to confirm its origin by direct measurements of I_σ/I_π. This is done by proving that the spectrum of a σ light is really composed of the frequencies corresponding to emission by the m = ±1 Zeeman sublevels, collisionally excited.

The experimental evidence for the presence of residual gases is obtained by putting in the detection beam absorption chambers containing high-purity odd isotopes ¹⁹⁹Hg or ²⁰¹Hg) of mercury. One can then verify that the spectrum of the I_σ signal has two components at $k_0 \pm \omega$. The sum of the amplitudes of the absorption signals gives directly $I_\sigma/I_\pi \simeq 10^{-3}$ (see Fig. 4), which from (27) is the value of g/Γ. When the filter is interposed in the excitation beam, no absorption signal is detected, thus proving that there is no direct excitation of the $m = \pm1$ Zeeman components by the lamp.
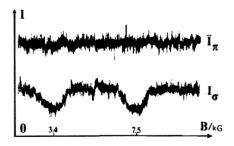

FIG. 4. Measurements of g/Γ at low mercury density ($N = 2\times10^{11}$ at./cm³) obtained with the magnetic scanning technique. The value of g/Γ is about 2×10^{-3}. The experiments are done with ¹⁹⁸Hg and ¹⁹⁹Hg filters at room temperature placed in the detection beam. Since $\bar{I}_\pi$ is not zero, the absorption of the π-fluorescence light by the ¹⁹⁸Hg filter is not total. Indeed, $\bar{I}_\pi$ represents about 10^{-3} of the incident π-fluorescence light, and is due essentially to residual stray light from the lamp. Each component of the σ-fluorescence light is nearly completely absorbed at the crossing points.

4. Residual-gas origin

The residual gases are due to H_2O-vapor desorption during the sealing operations on Pyrex tubes, and also to diffusion of helium through the silica walls $(T = 300\,^\circ K)$ of the cell.

Trapping operations are needed to fill a cell with mercury, as they permit the formation of a ring of condensed mercury and thus avoid great losses of a very expensive isotopic species. But during the sealing operations the traps are enriched with H_2O vapor and other gases from the Pyrex walls. It is especially this last operation on the cell which results in a large trapping of H_2O vapor and gives the 10^{-3} residual value for depolarization. Taking the values of Holland[21] and Dushman[22] for the volume of gases desorbed by a Pyrex wall, one obtains for a cell of 20 cm³ volume a residual-gas pressure of 2×10^{-3} Torr, assuming that all gases are trapped in the cell, which is in good agreement with observation.

In order to obtain cells for which $g/\Gamma < 10^{-4}$, we have modified the filling method slightly. When the mercury has condensed into a ring, we remove the trap and the sealing is done with mercury at room temperature. This results in big losses of mercury but in weak residual-gas pressures.

Measurements on a test cell have shown that He diffusion under our conditions is about 2×10^{-5} Torr a day, or 2×10^8 at./sec (for a cubic 2-cm cell with 1-mm-thick walls.) This suggests that the He pressure in the room is about ten times that commonly assumed under normal conditions.[23] We prevented much He diffusion by storing the cells between experiments in a high-vacuum Pyrex chamber. During the course of the experiments reported below, no increase of $g/\Gamma < 10^{-4}$ was seen.

5. Remarks

The value $g/\Gamma \sim 10^{-3}$ roughly corresponds to pressures of 10^{-3} Torr. For low temperatures we have verified that g/Γ is constant with the temperature of the cold point of the cell. Such a pressure for H_2O or He corresponds to the conditions of an unsaturated vapor. It is therefore hardly possible that residual gases are partially condensed in the measurements at low temperatures. The measured values of g/Γ are certainly correct at greater values of the temperature, under the conditions of the experiments.

A 10^{-3} residual depolarization effect at low temperature seems totally negligible. But so far as collisions with residual gases are concerned this gives at room temperature a very important parasitic effect due to the amplifying role of multiple scattering (Fig. 3) and a contribution to I_σ/I_π of the order of magnitude of that of resonant collisions. In fact, no significant experiments can be done under these conditions, as shown in Fig. 3 where the differences between the two curves represent the excitation transfer due to residual gases amplified by multiple scattering.

In contrast to the present experiments, which are very sensitive to small intensities of the fluorescent light, a 10^{-3} Torr residual-gas pressure is of no importance for Hanle-effect experiments; such a pressure will only increase the widths of the Hanle curves by about 10^{-2} of the total width, i.e. typically by $10^{-2}\,\Gamma$.

6. Conclusions

With the above-mentioned tests and verifications, one can conclude that I_σ/I_π measured with an appropriate cell $(g/\Gamma < 10^{-4})$ is given by (16) and represents the effect of excitation transfer between the $m = 0$ and $m = \pm 1$ Zeeman sublevels due to *resonant* Hg*-Hg *collisions*, without any parasitic contributions.

V. FURTHER REMARKS ON MULTIPLE SCATTERING

A theoretical and experimental report is being published on this issue,[6] and we limit our remarks here to a few qualitative ones. From (16), I_σ/I_π is a function of g^{10}, which depends on B, and of λ/Γ^σ, which does not. This last point has been investigated experimentally, although there is no *a priori* reason to suspect a field dependence of the parameters of multiple scattering for fields greater than 2 kG, i.e., once the splittings exceed the Doppler width.

The first investigation is based on Sec. IV C and Fig. 3. One can compare the values of I_σ/I_π obtained under the same experimental conditions (mercury densities) for cells containing residual gases at different pressures. As g^{10} and g are known, and since g may be shown to be field independent within 3% error by doing experiments at low temperature, one can deduce that the two curves of Fig. 3 differ by only a translation factor $\lambda g/\Gamma^\sigma$ which is field independent. Then λ/Γ^σ does not depend on the field strength within the experimental uncertainties of about 5%.

The second kind of investigation uses cells containing a rare gas at a pressure such that $g/\Gamma \gg 1$ and mercury density of about 2×10^{13} at./cm³. The σ and π intensities are then

$$I_\sigma \sim \lambda^{(1)}/(2\Gamma^\sigma + \Gamma^\pi), \quad I_\pi \sim \lambda^{(0)}/(2\Gamma^\sigma + \Gamma^\pi), \quad (28)$$

with[6]

$$I_\sigma/I_\pi = \lambda^{(1)}/\lambda^{(0)} \simeq 2$$

expressing quasithermal equilibrium for the ex-

cited state of the atoms. The experiment has been done with a 4 Torr xenon-mercury cell, showing that between 2 and 80 kG I_σ and I_π are field independent, and so the parameters of multiple scattering must be as well.

Note that if the field has bad inhomogeneity, one can observe a field dependence of Γ^σ due to the fact that between two successive reabsorptions of a σ photon, the field may differ by a quantity of the order of the Doppler width. Such effects cannot occur for π photons as the $m = 0$ Zeeman sublevel is not displaced by the field. Experimental evidence obtained under bad inhomogeneity conditions and Monte Carlo calculations of this effect are reported in Ref. 6.

VI. RESULTS

The measured field dependence of $\rho = I_\sigma/I_\pi$ at various mercury densities is given in Fig. 5 and reveals a very important decrease of ρ with the field. The decrease is due to the variations of the g^{10} collisional transfer rate as the energy difference between the levels is increased.

One can deduce from low-field measurements the values of $\lambda(N)/\Gamma^\sigma$, as g^{10}/Γ is known from previous experiments and theory.[7,10,15] For $N = 1.7 \times 10^{13}$ at./cm^3 one thus obtains $\lambda\Gamma/\Gamma_\sigma \simeq 39$. This is in fairly good agreement with the value $\lambda\Gamma/\Gamma^\sigma \simeq 40$ deduced from curves of Fig. 3 at the same mercury density and using the $g/\Gamma = 2 \times 10^{-3}$ value obtained from low-temperature data.

The variations of ρ between 3 and 77 kG are by about a factor of 3. The determination of the ρ value at fields lower than 3 kG is of no interest (as stressed in Sec. I), since the results may be af-
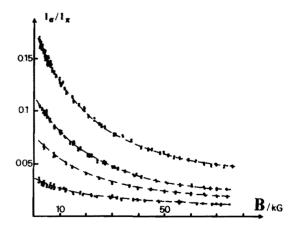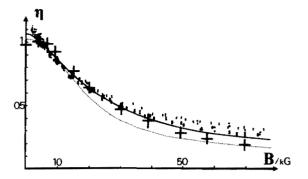

FIG. 6. Comparison of experimental and theoretical variations of $\eta(B)$, which is proportional to the $m = 0$ $\rightarrow m = \pm 1$ transfer rate. The experimental values are plotted for several densities ($\star$ for 2×10^{13} at.-cm^3, $\bullet$ for 1.7×10^{13} at./cm^3, and $*$ for 1.3×10^{13} at./cm^3) and exhibit a very small variation with N. The full curve represents the theoretical predictions (Refs. 10 and 17) obtained with R^{-3} dipole-dipole interaction. The dotted curve is the prediction without velocity averaging for $v = u = (2kT/M*)^{1/2}$. The crosses are the predictions obtained without velocity averaging with the formulation which uses the correlation function for R^{-3} dipole-dipole interaction.

fected by several parasitic effects. Multiple scattering for fields lower than 2 kG occurs in an intermediate regime where the σ and π photons are not diffused independently and thus give rise to depolarization. Moreover, the use of fields greater than 3 kG permits avoidance of possible (small) effects connected with direct excitation of the $m = \pm 1$ sublevels by photons belonging to the wings of the excitation profile and also of possible anomalous dispersion effects.[6]

In fact, as the theoretical variations of g^{10} with B are smaller than 5% between 0 and 3 kG, this is not a fundamental limitation of the study. But it may be for the g^{1-1} transfer rate, which varies by 20% in this field range.[10]

Under our experimental conditions, ρ depends linearly on g^{10}. To compare the field variations of g^{10} with theoretical predictions, one has to eliminate the $\lambda\Gamma/\Gamma^\sigma$ factor, which is not accurately known for all density values. This is done by normalizing the results at fixed density at the value for $B = 5$ kG. One then obtains:

$$\eta(B) = \rho(B)/\rho(5) = g^{10}(B)/g^{10}(5). \tag{29}$$

Note that though g^{10} is temperature dependent,[17] the experiments have been performed at fixed temperature in the cell ($T \simeq 25$°C) at various densities controlled by the temperature of the cold point of the cell.

As g depends linearly on N, η must be independent of the density N within the experimental un-

FIG. 5. Field variations of I_σ/I_π for a cell verifying $g/\Gamma < 10^{-4}$. Each curve corresponds to a different mercury density in the cell ($N = 2 \times 10^{13}$, 1.7×10^{13}, 1.3×10^{13}, and 9.5×10^{12} at./cm^3). Increasing with N, ρ decreases with B.

certainties. This is fairly well verified on the plot of Fig. 6, confirms the validity of our model and of the experimental conditions we have adopted to perform the experiments. Nevertheless, some systematic effects seem to exist for the lowest value of the density at strong fields, possibly due to a small uncorrected contribution from residual gases. In fact, the uncertainties in η due to the various corrections we have to perform are about 10%, about the magnitude of the dispersion of experimental measurements.

VII. COMPARISON OF EXPERIMENTAL AND THEORETICAL BEHAVIOR OF g^{10} WITH $\vec{B}$

Theoretical curves with and without velocity averaging are shown in Fig. 6. The hypotheses of the calculations are given in a previous paper,[10,17] the fundamental assumption being that the R^{-3} dipole-dipole interaction is responsible for the $m = 0 \rightarrow m = \pm 1$ excitation transfer.

A. Deduction of parameters for Hg* (6 $^3P_1$)-Hg collisions

The adiabaticity parameter τ_c for the problem[10,17] is given by

$$\tau_c = g_J \mu_B B / \omega_c ,$$

with

$$\omega_c = \left(\frac{2kT}{M^*}\right)^{3/4} \left(\frac{4k_0^3}{9\Gamma}\right)^{1/2} \left(\frac{8}{27}\right)^{-1/4} . \tag{30}$$

Then for $T = 300\,°K$ and $\omega_c = 20.3$ GHz

$$\tau_c = 1.023 \times 10^{-4} B \text{ (gauss)} ,$$

and $\tau_c = 1$ for $T = 300\,°K$ and $B = 9.77$ kG. We then normalize the theoretical values to the value at 5 kG to obtain the plots of Fig. 6.

B. Comparison with experimental results

The curve obtained without velocity averaging for $v = u = (2kT/M^*)^{1/2}$ overestimates the experimental variations. But the theoretical values after velocity averaging are in good agreement with the experimental results. Also note that the approxi-

mate solution obtained using the symmetrical correlation function for the potential[17,24] is in good agreement [for $v = u = (2kT/M^*)^{1/2}$] with the experimental results. After velocity averaging (which can be done analytically[25]) the rate of variation with the field will be slightly underestimated. This confirms that for such a problem, the method provides a simple means for estimating (sometimes accurately) the variations. As mentioned in a previous paper,[17] the role of detailed balance will be negligible in interpreting the results: the corrections are smaller than the experimental dispersion.

C. Conclusion

The use of strong magnetic fields, which permits a continuous variation of the energy difference between levels, thus offers the possibility of a detailed and reliable comparison between theory and experiment and a test of the validity of the interaction potential. In the particular case of Hg*(6^3P_1)-Hg(6^1S_0) collisions, one can conclude that R^{-3} dipole-dipole interaction is a good approximation for the potential over a 160-GHz energy range. The investigation of the field variations of the g^{1-1} transfer rate and a test of symmetry properties in the very simple and clear situation offered by Hg*(6^3P_1) would be of interest. But this requires a continuous tunable source at 2537 Å.

APPENDIX: EFFECTS OF FIELD ON $(6s, 6p)$ CONFIGURATION

The effect of a magnetic field on the $(6s, 6p)$ configuration of mercury (even isotopes) has been studied in various publications.[26-28] The eigenvectors in the $\{LSJM_J\}$ representation are given by

$$|\psi(^3P_1)\rangle = \alpha |111M\rangle - \gamma |101M\rangle ,$$

$$|\psi(^1P_1)\rangle = \gamma |111M\rangle + \alpha |101M\rangle .$$

The energies of the $^1P_1$, $^3P_2$, $^3P_1$, and $^3P_0$ states are respectively, written, E^1, E^2, E^3, and E^4. To study the perturbations of the $|^3P_1, M_J\rangle$ wave functions and energies by the field, a perturbative treatment is sufficient up to 200 kG. One then obtains

$$|\psi(^3P_1), M = \pm 1\rangle = |\psi(^3P_1), M = \pm 1\rangle - \frac{\alpha\omega}{2(E^3 - E^2)} |\psi(^3P_2), M = \pm 1\rangle \pm \frac{\omega}{2} \frac{\alpha\gamma}{E^3 - E^1} |\psi(^1P_1), M = \pm 1\rangle ,$$

$$|\psi(^3P_1), M = 0\rangle = |\psi(^3P_1), M = 0\rangle - \frac{\alpha\omega}{E^3 - E^2}\left(\frac{1}{3}\right)^{1/2} |^3P_2, M = 0\rangle - \frac{\omega\alpha}{E^3 - E^4}\left(\frac{2}{3}\right)^{1/2} |^3P_0, M = 0\rangle ,$$

and for the energies

$$E(^3P_1, M = \pm 1) = E^3 \pm \omega \left(1 + \frac{\alpha^2}{2} \right) + \frac{\alpha^2 \omega^2}{4} \left(\frac{\gamma^2}{E^3 - E^1} + \frac{1}{E^3 - E^2} \right) ,$$

$$E(^3P_1, M = 0) = E^3 + \frac{1}{3} \frac{\alpha^2 \omega^2}{E^3 - E^2} + \frac{2}{3} \frac{\alpha^2 \omega^2}{E^3 - E^4} ,$$

with $\alpha = 0.985$ and $\gamma = 0.171$.[26]

With A the fine structure constant, one can show that the displacement of the $M = 0$ Zeeman sublevel is of the order of $\frac{1}{2}\omega^2/A$, and of about 0.1 GHz for $B = 80$ kG and 0.7 GHz for $B = 200$ kG. The difference to Zeeman approximation for the energy of the $M = \pm 1$ sublevels is $\frac{1}{8}\omega^2/A$, which is always negligible under our experimental conditions.

The lifetime associated with the M Zeeman sublevel described by the $|\varphi(M)\rangle$ wave function is inversely proportional to $|\langle 6^1S_0 | \vec{P} | \varphi(M)\rangle|^2$. Then the relative modification of the lifetime of the M (6^3P_1) Zeeman sublevel is $\omega\alpha^2/(E^3 - E^1)$. This correction, linear in the field because of the mixing of 6^3P_1-6^1P_1 wave functions is about 6×10^{-4} for $B = 200$ kG, and is of opposite sign for the $M = \pm 1$ sublevels. To this order of the calculation the lifetime of the $M = 0$ sublevel is not modified. One can remark that all these effects are completely negligible for our experimental investigations, and also that the $|^3P_0\rangle$ and $|^3P_2, M \neq \pm 2\rangle$ states now have a finite lifetime,[27] proportional to $1/B^2$, of about $10^{-2} s$ for $B \sim 200$ kG.

*Present address: Universitat Marburg, R. F. A.

†Associé au CNRS—LA No. 18.

[1] J. C. Gay and W. B. Schneider, J. Phys. Lett. 36, L185 (1975).

[2] A. Omont, thesis, University of Paris, 1961 (unpublished).

[3] A. Omont and J. Brossel, C. R. Acad. Sci. 252, 710 (1961).

[4] F. Quarré, thesis, University of Paris, 1967 (unpublished).

[5] M. Crance, thesis, University of Paris, 1968 (unpublished).

[6] J. C. Gay and A. Omont (unpublished).

[7] A. Omont and J. Meunier, Phys. Rev. 169, 92 (1968).

[8] M. I. Dyakhonov and V. I. Perel, Sov. Phys. JETP 21, 227 (1965).

[9] P. R. Berman and W. E. Lamb, Phys. Rev. 187, 221 (1969).

[10] J. C. Gay, J. Phys. (Paris) 37, 1135 (1976).

[11] J. P. Faroux, thesis, University of Paris, 1969 (unpublished).

[12] J. C. Gay, J. Phys. (Paris) 37, 1165 (1976).

[13] E. B. Saloman and W. Happer, Phys. Rev. 160, 23 (1967).

[14] B. M. Dodsworth, J. C. Gay, and A. Omont, Phys. Rev. A 3, 1912 (1971).

[15] B. M. Dodsworth, J. C. Gay, and A. Omont, J. Phys. (Paris) 33, 65 (1972).

[16] T. Holstein, Phys. Rev. 72, 1212 (1947).

[17] J. C. Gay and W. B. Schneider, preceding paper, Phys. Rev. A 20, 879 (1979).

[18] J. C. Gay, thesis, University of Paris, 1976 (unpublished).

[19] J. Butaux, thesis, University of Paris, 1972 (unpublished).

[20] B. Fuchs, W. Hanle, W. Oberheim, and A. Scharmann, Phys. Lett. 50, 337 (1974).

[21] L. Holland, Properties of Glass Surfaces (Chapman and Hall, London, 1966).

[22] S. Dushman, Scientific Foundations of Vacuum Technique (Wiley, New York, 1962).

[23] F. J. Norton, J. Appl. Phys. 46, 34 (1975).

[24] A. Omont, thesis, University of Paris, 1967 (unpublished).

[25] A. Omont, J. C. Msieh, and J. C. Baird, Phys. Rev. A 6, 152 (1972).

[26] R. Kohler, and P. Thaddeus, Phys. Rev. 134, A1204 (1964).

[27] D. Vienne, M. C. Bigeon, and J. P. Barrat, Opt. Commun. 6, 261 (1972).

[28] E. Luc-Koenig, J. Phys. B 7, 1052 (1974).